Determination of 3-Hydroxy-3-methylglutaryl CoA Reductase Activity in Plants

Narciso Campos, Montserrat Arró, Albert Ferrer, and Albert Boronat

Abstract

The enzyme 3-hydroxy-3-methylglutaryl CoA (HMG-CoA) reductase catalyzes the NADPH-mediated reductive deacylation of HMG-CoA to mevalonic acid, which is the first committed step of the mevalonate pathway for isoprenoid biosynthesis. In agreement with its key regulatory role in the pathway, plant HMG-CoA reductase is modulated by many diverse external stimuli and endogenous factors and can be detected to variable levels in every plant tissue. A fine determination of HMG-CoA reductase activity levels is required to understand its contribution to plant development and adaptation to changing environmental conditions. Here, we report a procedure to reliably determine HMG-CoA reductase activity in plants. The method includes the sample collection and homogenization strategies as well as the specific activity determination based on a classical radiochemical assay.

Key words 3-Hydroxy-3-methylglutaryl CoA reductase, HMG-CoA reductase, HMGR, MVA, Mevalonate pathway, Isoprenoid, Terpenoid

1 Introduction

1.1 Molecular Properties of Plant HMG-CoA Reductase

HMG-CoA reductase (HMGR) (EC 1.1.1.34) catalyzes the first committed step of the mevalonate pathway for isoprenoid biosynthesis, consisting in the NADPH-mediated reductive deacylation of HMG-CoA to mevalonic acid [1] (Fig. 1). The enzyme exerts a key regulatory role on the flux of the mevalonate pathway in all eukaryotes [2–4] and in plants is critical not only for normal growth and development but also for the adaptation to diverse challenging conditions [4]. Plant HMGR is controlled at transcriptional and posttranslational levels in response to many developmental and environmental signals such as phytohormones, calcium, calmodulin, light, wounding, elicitor treatment, and pathogen attack [5, 6]. In all plants studied so far, HMGR is encoded by a multigene family [7]. Some HMGR genes participate in general house-keeping roles such as sterol biosynthesis, whereas others are required for more specific developmental or adaptive

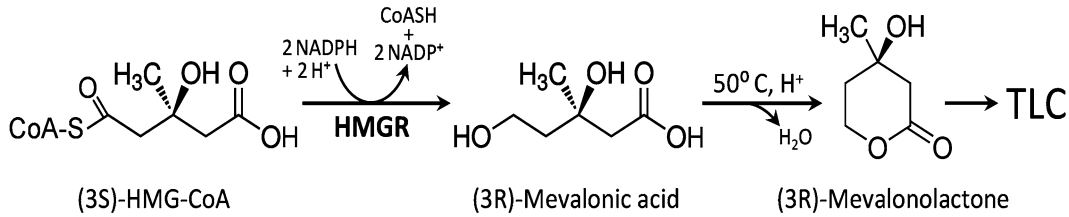

Fig. 1 The HMGR activity assay. Eukaryotic HMGR catalyzes the stereospecific NADPH-dependent reductive deacylation of (3S)-HMG-CoA to (3R)-mevalonic acid [1]. The HMGR assay reaction product is subsequently converted to mevalonolactone by heating in acid medium. The heat treatment also hydrolyses HMG-CoA to free HMG acid and CoASH. The mevalonolactone is more hydrophobic than the HMG acid or any remaining HMG-CoA and separates well from these compounds in the TLC system

processes [4]. This scenario anticipates a complex transcriptional control by multiple regulatory circuits [8]. In addition, posttranslational control of plant HMGR has been proposed to occur in response to light [9, 10], salt stress [11], or alteration of the metabolic flux through sterol or sphingolipid biosynthetic pathways [12, 13]. Protein degradation [10, 11], inhibition [14] or activation by calcium [15], and phosphorylation at a conserved site of the catalytic domain [16–18] are mechanisms by which plant HMGR is posttranslationally modulated. Protein phosphatase 2A (PP2A) has been identified both as a transcriptional and a posttranslational regulator of HMGR in *Arabidopsis* [11]. The interaction with HMGR occurs through a B" PP2A regulatory subunit, which is also a calcium-binding protein [11]. These observations uncovered the potential of PP2A to integrate developmental and Ca^{2+}-mediated environmental signals in the control of plant HMGR [19]. Because plant HMGR may be affected by many diverse stimuli, a careful control of the plant growth and sample collection conditions is critical to attain reproducibility in its activity determination.

Plant HMGR is an endoplasmic reticulum (ER) protein of about 63–70 kDa. *Arabidopsis* and tomato HMGR have been shown to span the ER membrane twice [20–22]. Both the N-terminal region and the highly conserved catalytic domain are in the cytosol, whereas only a short stretch of the protein is in the ER lumen. Insertion in the ER membrane is mediated by the Signal Recognition Particle (SRP) that recognizes the two hydrophobic sequences which will become membrane spanning segments [20]. Since these two sequences are highly conserved, it was proposed that all plant HMGR variants are primarily targeted to the ER [20]. However, in *Arabidopsis* and tobacco cells, HMGR also localizes in still uncharacterized bodies that range between 0.2 and 2.0 μm in diameter [23, 24]. HMGR was purified as a dimer or tetramer with subunits of 55–45 kDa from potato [25], *Hevea* [26], and radish [27] which, according to the corresponding nucleotide sequences [28–30], may correspond to the protease-released

catalytic portion. This is in agreement with the previous crystallization of human HMGR catalytic domain as a tetramer, with each active site (four in total) formed in the interphase of two neighboring HMGR subunits [31]. Thus, the available data indicate that not only the sequence of the catalytic domain of HMGR but also its quaternary structure is conserved in high eukaryotes.

1.2 Setting Up the HMG-CoA Reductase Activity Assay

Plant HMGR activity was first detected in 1967, in *Hevea brasiliensis* latex [32], and demonstrated at high levels in the same system 2 years later [33]. In the 1970s, different methods to determine HMGR activity were set up in pea seedlings [34], sweet potatoes [35], anise cell line [36], tobacco seedlings [37] and etiolated radish seedlings [38]. This pioneer work uncovered some common biochemical properties of plant HMGR, that have allowed the detection of its enzymatic activity in many different organs, tissues, cell lines or extracts of 40 plant species (Table 1). When plants are submitted to homogenization and centrifugation, the HMGR activity is detected in the final microsomal pellet (about 100,000 × *g*), as it would be expected from its ER localization, but also in the sediment obtained at low centrifugation forces (1,500–16,000 × *g*) [5, 39] (Table 1). Therefore, a crude extract, instead of a more elaborated subfraction, may be required to measure total HMGR activity. Alternatively, plant HMGR has been released from the insoluble fraction by extraction with a nonionic detergent [27, 40] or by intended proteolytic digestion [25]. Higher levels of potato HMGR activity were obtained in the presence of cysteine, serine and threonine peptidase inhibitors [6, 10], indicating that these should be included in the homogenization buffer to recover the total HMGR activity.

The catalytic activity of plant HMGR depends on free thiol groups and a reducing agent has been used to protect their reduced state [41, 42]. It was reported that DTT is better than 2-mercaptoethanol or glutathione for this purpose [34, 43]. Maximal HMGR activity occurs at pH 7.3–7.5 in radish [27] and sweet potato [42], and about pH 6.8 in Hevea latex [40, 41]. In pea [14] and guayule [44], two pH optima were found, corresponding to HMGR from the heavy or the light fractions: 7.9 and 6.9, respectively, in the case of pea, and 7.5 and 7.0, respectively, in the case of guayule. HMGR activity was assayed in phosphate buffer in all the above systems, but in *Arabidopsis* we found that the Hepes-KOH buffer system is also suitable. Ethylenediaminetetraacetic acid (EDTA) is used in most of the above-mentioned methods. It was proposed to inhibit the subsequent reactions of the mevalonate pathway in Hevea latex [33] and was found to increase the apparent HMGR activity in sweet potato extracts [42].

In most cases, HMGR activity has been detected in plant extracts by a [^{14}C]HMG-CoA-based radiochemical method, which

Table 1
List of plants where HMGR activity has been measured. Only the earliest report for each particular case (plant species, organ, tissue, cell culture and subcellular fraction) is indicated. Pellet (P) and supernatant (S) fractions obtained by differential centrifugation appear with the corresponding gravitational force (g), as a suffix

Species	Organ/tissue	Fraction	References
Arabidopsis thaliana	Rosette leaf	S_{200}	[58]
	Fully expanded leaf	S_{200} and $P_{16,000}$	[57]
	Green seedling	S_{200}	[12]
	Dry seed	S_{200}	[56]
	Seedling aerial part and root	S_{200}	[11]
Arachis hypogaea	Green seedling	$P_{105,000}$	[60]
Artemisia annua	Leaf	$P_{105,000}$	[61]
Bixa orellana	Callus, leaf	$P_{100,000}$	[62]
Brassica napus	Developing seed	P_{1200} and S_{1200}	[63]
Cannabis sativa	Leaf	$S_{24,000}$	[50]
Cucumis melo	Fruit pericarp	$P_{50,000}$	[64]
Daucus carota	Cell culture	$P_{10,000}$ and $P_{105,000}$	[65]
Dunaliella salina	Cell culture (entire organism)	Low speed pellet (?)	[66]
Euphorbia lathyris	Latex, leaf, stem	S_{500} and $P_{18,000}$	[67]
	Latex	$S_{5,000}$ and $P_{5,000}$	[68]
Glycine max	Seedling apical part, cotyledon, hypocotyl and root, cell culture	$P_{5,000}$ and $P_{100,000}$	[69]
Gossypium barbadense	Stele tissue	$P_{105,000}$	[70]
Gossypium hirsutum	Stele tissue	$P_{105,000}$	[70]
Helianthus tuberosus	Tuber explants	$P_{15,000}$ and $P_{105,000}$	[71]
Hevea brasiliensis	Latex	$S_{20,000}$	[32]
	Latex	P_{600}	[33]
Hordeum vulgare	Seedling	$P_{16,000}$ and $P_{105,000}$	[72]
Ipomoea batatas	Root	$P_{105,000}$	[35]
Lithospermum erythrorhizon	Cell culture	$P_{10,000}$ and $P_{100,000}$	[73]
	Hairy root	$S_{100,000}$ and $P_{100,000}$	[74]
Malus x domestica	Fruit skin	$S_{105,000}$ and $P_{105,000}$	[75]
Medicago sativa	Hairy root	$P_{100,000}$	[53]
Nepeta cataria	Leaf, callus tissue	$P_{2,000}$ and $P_{100,000}$	[76]
Nicotiana benthamiana	Leaf	$S_{13,000}$	[77]

(continued)

Table 1
(continued)

Species	Organ/tissue	Fraction	References
Nicotiana tabacum	Aerial part of seedling	$P_{200,000}$	[37]
	Cell culture KY-14	$P_{10,000}$ and $P_{100,000}$	[78]
	Seedling, fully expanded leaf, Callus	$P_{100,000}$	[79]
	Cell culture BY-2	$P_{100,000}$	[13]
	Developing seed	$P_{1,200}$ and $S_{1,200}$	[63]
Ochromonas malhamensis	Cell culture (entire organism)	$P_{145,000}$	[80]
Parthenium argentatum	Fully expanded leaf	$S_{45,000}$ and $P_{2,500}$	[44]
	Bark of lower stem	$P_{105,000}$	[81]
Persea americana	Fruit mesocarp	$P_{27,000}$	[82]
	Seed	$P_{27,000}$	[83]
Phaseolus radiatus	Leaf	$P_{2,500}$	[84]
Picea abies	Seedling, leaf, callus, cell culture	$P_{18,000}$ and $P_{105,000}$	[85]
Pimpinella anisum	Cell culture	Particulate fraction (?)	[36]
Pisum sativum	Etiolated seedling, green seedling	Crude extract, $P_{2,000}$, $P_{10,000}$ and $P_{105,000}$	[34]
Raphanus sativus	Seedling	$P_{16,000}$ and $P_{105,000}$	[38]
Salvia miltiorrhiza	Hairy root	(?)	[48]
Sinapis alba	Green seedling	$S_{200,000}$ and $P_{120,000}$	[86]
Solanum lycopersicum	Fruit, leaf	$S_{105,000}$ and $P_{3,500}$	[87]
Solanum tuberosum	Tuber tissue	$P_{105,000}$	[88]
Solanum xantocarpum	Cell suspension culture	$S_{4,000}$	[89]
Spinacia oleracea	Leaf	$P_{120,000}$	[90]
Stevia rebaudiana	Leaf	$P_{1,500}$ and $P_{105,000}$	[91]
Taraxacum brevicorniculatum	Latex	Crude extract	[92]
Zea mays	Etiolated seedling	$P_{140,000}$	[93]

has thus become classical in this context (Table 1). The assay involves the separation of the reaction product from the labeled substrate by thin layer chromatography (TLC) [43, 45, 46] or organic solvent extraction [47]. To optimize separation, mevalonic acid is first converted to its less hydrophilic derivative mevalonolactone (Fig. 1). Alternative non-radiochemical methods for HMGR

activity determination have also been reported. They include the far less sensitive, but simpler, spectrophotometric assay based on monitoring the conversion of NADPH into $NADP^+$ [48–51] and others, still less sensitive than the radiochemical method, using HPLC [52, 53] or liquid chromatography-tandem mass spectrometry [54]. Only the later has not been applied to plants. Analysis done in *Arabidopsis* showed a direct correlation between the HMGR activity levels determined by the radiochemical method and the percentage of seedlings that develop true leaves (achieve seedling establishment) in the presence of the HMGR-specific inhibitor mevinolin [11, 55]. Thus, the HMGR activity measured in plant extracts faithfully represents the HMGR catalytic potential existing in vivo [55].

The above studies allow a well-reasoned design of protocols for plant HMGR extraction and activity determination. The method we report was set up in *Arabidopsis* [11, 56, 58] (Table 1), but should be applicable with minor variations to other plants.

2 Materials

2.1 Reagents and Solutions

Prepare all solutions with ultrapure water (17 MΩ resistivity at 25 °C). Unless otherwise stated, use analytical grade reagents.

1. HCl: 25 % in H_2O. Dilute the 37 % commercial stock 25:12 with H_2O. Store at room temperature.
2. Radioactive ink. Dilute about 1 μCi [^{14}C]-HMG-CoA (*see* **item 18**) in 100 μL of India ink. Store at room temperature.
3. Cytoscint scintillation cocktail (MP Biomedicals). Store at room temperature.
4. Triton X-100: 20 % (v/v) in H_2O. Store at 4 °C.
5. Ethylenediaminetetraacetic acid (EDTA): 500 mM in H_2O, pH 7.5. Add EDTA powder to H_2O and dissolve by adding NaOH pellets to the stirring suspension. Finish pH adjustment with NaOH 1 M and bring to the final volume. Store at 4 °C.
6. Tris–HCl, pH 7.5: 20 mM in H_2O. Store at 4 °C.
7. Bio-Rad Protein Assay dye reagent concentrate (Bio-Rad). Store at 4 °C.
8. HKS buffer: 40 mM Hepes, pH 7.2 (*see* **Note 1**), 50 mM KCl and 100 mM sucrose. Dissolve reagents in H_2O, equilibrate pH with KOH and adjust the volume. Aliquot and store at −20 °C. Keep the thawed aliquot at 4 °C up to 2 weeks.
9. Aprotinin (Sigma): 3 mg/mL in HKS buffer. Store at −20 °C.
10. Leupeptin (Sigma): 4 mg/mL in HKS buffer. Store at −20 °C.
11. Trans-epoxysuccinyl-L-leucylamindo-(4-guanidino)-butane (E-64) (Sigma): 3 mg/mL in HKS buffer. Store at −20 °C.

12. Pepstatin (Sigma): 3 mg/mL in methanol. Store at –20 °C.
13. Bovine Serum Albumin (BSA) protein concentration standards (0.1–0.6 mg/mL). Store at –20 °C.
14. DTT: 1 M in H_2O. Store at –80 °C.
15. DL-3-Hydroxy-3-methylglutaryl coenzyme A (HMG-CoA) (Sigma) (*see* **Note 2**): 4 mM in 50 mM KH_2PO_4 pH 4.5. Store at –80 °C.
16. Yeast glucose 6-phosphate dehydrogenase (G6P-DH) (Sigma): 1 U/µL in HKS buffer. Aliquot and store at –80 °C; thaw only once.
17. TGNB solution: 158 mM glucose 6-phosphate (G6P) (Roche), 7.9 mM NADP (Roche) and 1.58 mg/mL BSA. Weight and dissolve reagents in 658 mM Tris–HCl, pH 7.2. Aliquot and store at –80 °C. The TGNB solution, together with G6P-DH (*see* **item 16**), will constitute the NADPH regeneration system.
18. Hydroxy-3-methylglutaryl Coenzyme A, DL-3-[Glutaryl-3-^{14}C]-, 50 µCi (1.85 MBq) (0.02 mCi/mL, 40–60 mCi/mmol) ([^{14}C]-HMG-CoA, CAS Number: 103476-21-7) (PerkinElmer) (*see* **Note 2**). Aliquot and store at –80 °C.
19. Phenylmethylsulphonyl fluoride (PMSF) (Sigma). Aliquot in microcentrifuge tubes (about 5–15 mg per tube) and store at room temperature. Just before use, dissolve the aliquot in isopropanol at 20 mg/mL.
20. HM buffer (homogenization buffer): 40 mM Hepes-KOH, pH 7.2, 50 mM KCl, 100 mM sucrose, 16 mM EDTA, 0.2 % (v/v) Triton X-100, 10 mM DTT, 15 µg/mL aprotinin, 20 µg/mL leupeptin, 4.2 µg/mL E-64, 1.8 µg/mL pepstatin A, and 100 µg/mL PMSF. Prepare just before use. For 5 mL of HM buffer, add the following stocks in the indicated order: 4.655 mL HKS buffer, 160 µL EDTA, 50 µL Triton X-100, 50 µL DTT, 25 µL aprotinin, 25 µL leupeptin, 7 µL E-64, 3 µL pepstatin A, and 25 µL PMSF. Mix immediately after PMSF addition and keep on ice.
21. Reaction cocktail (RC): 547 mM Tris–HCl pH 7.2, 131 mM G6P, 6.6 mM NADP, 1.3 mg/mL BSA, 15.6 mM DTT, 87.5 µM HMG-CoA, 38.36 µM (1,295 Bq) [3-^{14}C]-HMG-CoA, and 0.35 U yeast G6P-DH. Just before use, prepare sufficient volume of RC for the total number of samples to be assayed (16 µL per assay), keeping the following proportions: 13.3 µL TGNB, 0.25 µL DTT, 0.35 µL HMG-CoA, 1.75 µL [^{14}C]-HMG-CoA, and 0.35 µL G6P-DH. Mix and keep on ice.

2.2 Equipment

1. Polypropylene tubes (50 mL).
2. Racks and appropriate containers for liquid nitrogen.
3. Eppendorf Safe-Lock micro test tubes™. Alternatively, any other good quality microcentrifuge tube that withstand freezing

in liquid nitrogen and shaking in TissueLyser (Qiagen) (*see* **item 6**).

4. Cane for 5 NUNC cryo vials (MTG—Medical Technology Vertriebs).
5. Stainless steel beads 5 mm (Qiagen). Alternatively, stainless steel beads of similar diameter, from any local supplier. Clean the beads twice with H_2O, several times with acetone, until no dirt is released, and twice with 96 % ethanol. Dry the beads at 200 °C.
6. TissueLyser (Qiagen). Alternatively, use mortar and pestle.
7. Refrigerated microcentrifuge (*see* **Note 3**).
8. TLC plates (20×20 cm) made of silica gel 60 on plastic support (Merck).
9. TLC chamber with vertical grooves on the transverse walls.
10. Scotch® Magic™ Removable Tape 811.
11. Fujifilm™ BAS-MS Imaging Plate 20×40 cm (Fisher Scientific). Alternatively, any phosphor imaging screen of similar size to detect ^{14}C isotope emission.
12. Cassette for the 20×40 cm imaging plate. It should contain a separate plastic board, to stick TLC plates.
13. A storage phosphor imaging system (PhosphorImager™, Storm™, Typhoon™ or similar) to scan the exposed imaging plate.
14. Long, fine scissors (*see* **Note 4**).
15. Plastic 20 mL scintillation counting vials.
16. Liquid Scintillation β-counter.
17. ELISA plates and ELISA plate reader.

3 Methods

3.1 Sample Collection and Storage

1. Establish sample collection conditions and adhere to these conditions to keep reproducibility. In particular, collect plants or plant organs at a fixed time of the day and freeze them immediately after removal from their growing place. Be particularly expeditive when collecting in the dark growth period, since this may imply plant exposure to light.
2. Fill 50 mL polypropylene tubes with liquid nitrogen and place them in a stainless steel rack inside a proper container filled with liquid nitrogen.
3. Deep freeze the samples by placing them into the 50 mL polypropylene tubes. Let the liquid nitrogen to evaporate, till only few milliliters are left. Then, break plant samples into

small pieces with a spatula. Store the tubes unfastened at –80 °C until their liquid nitrogen evaporates completely.

4. Transfer 100–200 mg of the crumbled tissue to a pre-weighed microcentrifuge tube with a deep frozen spatula (*see* **Note 5**). Be fast to avoid sample thawing. Add a nitrogen-frozen stainless steel bead and close the microcentrifuge tube. Repeat this sequence for all samples (*see* **Note 6**).
5. Crush samples in a TissueLyser to obtain a fine powder (*see* **Notes 7** and **8**). Knock the tubes softly with a spatula or forceps to bring the powder to the bottom. Process samples immediately or store them at –80 °C (*see* **Note 9**).

3.2 Extract Preparation

1. Add 2 µL of homogenization buffer per mg of frozen tissue. Knock down the tube on the bench to facilitate a fast penetration of the buffer. Invert the tube several times to thaw the sample completely and put it on ice immediately afterwards. Do not process more than two tubes at once to avoid sample thawing in the absence of buffer. Keep the samples on ice until all of them are ready.
2. Invert all tubes once again (*see* **Note 10**). Centrifuge samples at 200 × *g* and 2 °C for 10 min. Brake down slowly to avoid sediment resuspension. Recover the supernatant (S_{200}) carefully with a micropipette and transfer it to a new tube.
3. Centrifuge again, in the same conditions, to remove the sediment completely. Keep the tubes with the clean S_{200} extract on ice.

3.3 HMGR Activity Assay

1. Dispense 26 µL of the extract at the bottom of a fresh microcentrifuge tube and 16 µL of RC (*see* **Note 11**) in the inside side of the lid. Pipette with care such that all the whole volume is released. Close the tube carefully. No RC liquid should fall down at this step. Let the tube on ice. Blanks should contain 26 µL of HM buffer instead of plant extract.
2. When all samples are ready, start the reaction by a short centrifuge pulse, just enough to bring the RC to the bottom, avoiding pellet formation (about 6,000–8,000 rpm in a microcentrifuge for few seconds). Immediately after the pulse, mix each sample by gentle vortexing. Incubate at 37 °C for 30–60 min (*see* **Notes 12** and **13**).
3. Stop the reaction by precipitation with acid (*see* **Note 14**). Pipette 7 µL of 25 % HCl solution in the inside side of the lid and close carefully. When all tubes are ready, centrifuge for few seconds to bring the HCl to the bottom. Vortex immediately after the pulse (*see* **Note 15** for **steps 1–3**).
4. Incubate at 50 °C for 10 min, to lactonize mevalonate.
5. Complete precipitation by incubating on ice for at least 10 min (*see* **Note 16**).

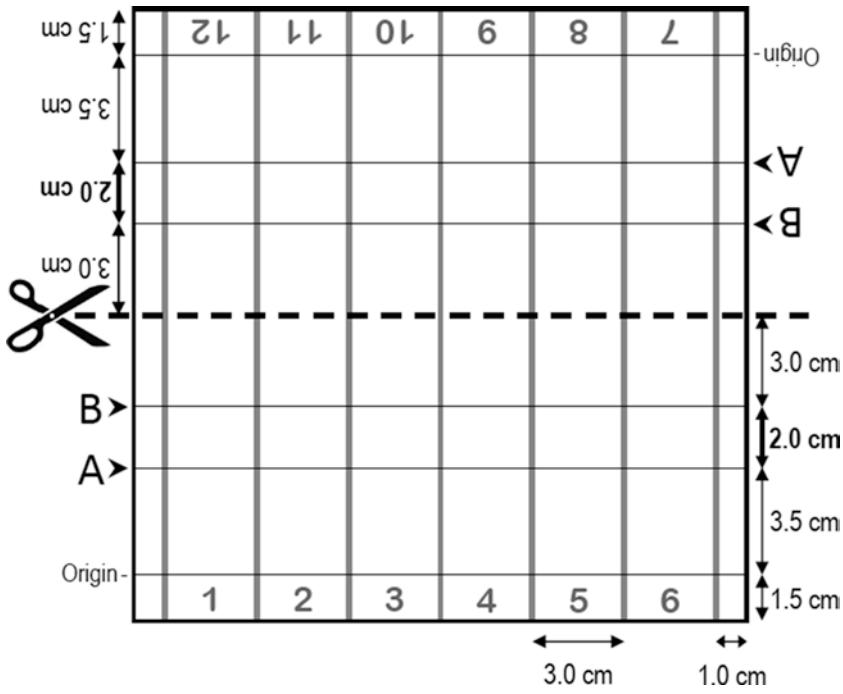

Fig. 2 Preparation of TLC plates for HMGR activity assays. A design to analyze up to twelve samples per 20 × 20 cm silica gel plate is shown. First, *horizontal* and *vertical lines* are drawn with a soft-tip pencil, as indicated in the figure. Next, a separation between lanes (*vertical gray lines*) are made by scoring the plate from top to bottom, displacing a pipette tip along a ruler. Removal of the silica gel avoids sample cross-contamination during the run. Finally, the plate is cut in two halves 10 × 20 cm in size. After the run, the mevalonolactone band will be positioned between *lines A* and *B* of the half-plate

6. Centrifuge at maximum speed for 5 min, at room temperature, to obtain a protein-free supernatant containing the mevalonolactone.

3.4 TLC and Radioactive Counting

1. Prepare TLC plates as indicated in Fig. 2.
2. Place the TLC plate on a double-block heater at 85 °C under the hood, with the silica gel facing up, and put a heavy flat object (i.e., a plastic rack) on the plate bottom to avoid curling and ensure full contact with the metal blocks (*see* **Notes 17** and **18**).
3. Streak the sample supernatant along the origin line. Do several applications for a total of 40 μL per sample and let the liquid dry before re-pipetting in the same surface. Keep the application band as thin as possible. It should not exceed 4–5 mm wide.
4. When all samples have been applied, let the plate cool down to room temperature. Make sure that all samples dry completely.
5. Prepare 100 mL of the eluent by adding 50 mL each of acetone and benzene (1:1) into the TLC chamber. Close the chamber and mix softly (*see* **Note 19**).

6. Place the plates into the chamber, with their lateral borders between the vertical grooves (*see* **Note 20**). Be fast and close the chamber immediately. Run chromatography for 18–20 min, just until the eluent reaches the upper border.
7. Remove plates from the chamber and let them dry for 5 min.
8. Mark plate lines A and B near the plate edges (outside the chromatography tracks, Fig. 2), with a spot of radioactive ink, using a needle or toothpick (*see* **Note 21**).
9. Fix the plates to the cassette board with removable tape (stuck behind the plates) and cover the plates with transparent plastic foil wrapped behind the board (*see* **Note 22**).
10. Fit the sandwich in an autoradiography cassette, together with a sensitive screen. Expose at room temperature for 12–36 h.
11. Read the imaging plate in a phosphor imaging system and print a copy in its true dimensions. Evaluate whether the mevalonolactone band is between lines A and B and whether the closely migrating by-product is outside this region (Fig. 3) (*see* **Note 23**). Otherwise, correct the line positions upwards or downwards, using the image of the radioactive ink marks as a reference.
12. Cut rectangular pieces of the TLC plate (3 cm wide, 2 cm high) containing the mevalonolactone band of each lane with long scissors.
13. Place each silica gel piece into a 20 mL counting vial by bending its plastic support. Fit the rectangular piece to the bottom

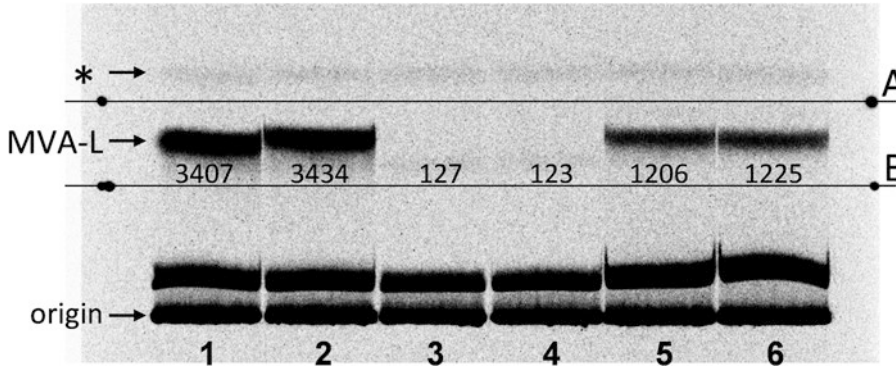

Fig. 3 Chromatogram of the HMGR assay reaction products. Two replicas from two samples (*lanes 1, 2* and *5, 6*, respectively) and a blank (*lanes 3, 4*) were applied at the bottom of the plate (origin). After migration, the TLC plate was exposed to a phosphor imaging screen, for 18 h. The radioactive spots drawn in the plate borders (**step 8** of Subheading 3.4) were used to confirm that the mevalonolactone band (MVA-L) ($R_f = 0.57$) was between the reference *lines A* and *B* (**step 11** of Subheading 3.4). The plate fragments delimited by these lines were processed for radioactivity counting. Notice that a weak side reaction product ($R_f = 0.77$, *asterisk*) migrating ahead of the mevalonolactone band was not included in the cut fragment. The number below each mevalonate band indicates the corresponding radioactive counts (cpm). Under our conditions, the assay replicas did not usually differ more than a 5 %

and add 10 mL of scintillation cocktail. The liquid should cover the TLC plate fragment completely.

14. Prepare a counting vial with 16 µL of RC, in duplicate, to determine the total number of counts per assay.
15. Keep vials in the dark at room temperature for 12–24 h to completely extract the mevalonolactone from the silica gel. Count samples with an appropriate ^{14}C program in a liquid scintillation β-counter (*see* **Note 24**).

3.5 Specific Activity Determination

1. Set an ELISA plate with 90 µL of H_2O per well (*see* **Note 25**).
2. Predilute plant extract with 20 mM Tris–HCl pH 7.5 (*see* **Note 26**).
3. Pipette 10 µL of the diluted plant extracts or BSA standards in the corresponding wells (*see* **Note 27**).
4. Predilute the concentrated Bradford reagent 2.5-fold with H_2O.
5. Dispense 100 µL of the diluted Bradford reagent to the ELISA plate wells with a multichannel pipette. Mix by pipetting up and down a few times avoiding bubble formation, until solution is homogenous, (*see* **Note 28**).
6. Measure absorbance at 595 nm in an ELISA plate reader, 30 min after protein and Bradford reagent mixing (*see* **Note 29**).
7. Calculate the HMGR specific activity in units per mg of protein extract. One HMGR unit is defined as the activity that converts 1 pmol of HMG-CoA into MVA per min at 37 °C. The HMGR specific activity can be calculated with the following formula:

$$\frac{\left(\mathrm{Cpm_s} - \mathrm{Cpm_b}\right)\cdot T_\mathrm{H}\cdot V}{\mathrm{Cpm_{RC}}\cdot V'\cdot t\cdot V_\mathrm{ext}\cdot P_\mathrm{c}},$$

where:

$\mathrm{Cpm_s}$: Counts per min incorporated into MVA in the sample.

$\mathrm{Cpm_b}$: Counts per min determined in the blank.

T_H: Total HMG-CoA substrate (labeled plus unlabeled) per assay, in pmol.

V: Total assay volume after HCl addition (49 µL in the above protocol).

$\mathrm{Cpm_{RC}}$: Total counts per min present in the assay (sample prepared in **step 14** of Subheading 3.4).

V': Assay volume applied to the TLC plate (40 µL in the above protocol).

t: Incubation time, in min.

V_ext: Plant extract volume added to the assay, in µL (26 µL in the above protocol).

P_c: Protein concentration of the plant extract, in mg per µL.

4 Notes

1. Buffer 40 mM H_2KPO_4 pH 7.2 can be used, instead of 40 mM Hepes-KOH pH 7.2, to determine HMGR activity in *Arabidopsis*.
2. Note that the HMG-CoA and [^{14}C]-HMG-CoA available stocks are racemic mixtures of the two possible stereoisomers. Since only the (3S)-HMG-CoA isomer will be processed by HMGR (Fig. 1), the effective concentration of the labeled and the unlabelled HMG-CoA will be half of the one indicated in the corresponding vials. This should be kept in mind in any calculation of substrate-dependent kinetic constants. The total HMGR activity of the plant sample will be also likely affected by the presence of the (3R)-HMG-CoA isomer, which was shown to be a competitive inhibitor of rat liver HMGR [59]. The rat liver HMGR activity was 1.8- to 2.0-fold higher with pure (3S)-HMG-CoA than with (3RS)-HMG-CoA racemic mixture [59].
3. A slow-down braking option in the centrifuge is important to have a good separation between supernatant and pellet in **steps 2** and **3** of Subheading 3.2.
4. The longer the scissors, the easier to cut the silica gel plate without border scrapping.
5. A spatula with capacity to transfer about 100 mg of tissue in a single step is advisable. We built such a device by bending the bottom end of an aluminum cryopreservation cane (*see* Subheading 2.2, **item 4**). The modified end just fitted into the round opening of the microcentrifuge tube.
6. The microcentrifuge tubes can be kept frozen by standing inside a metal block (of a common dry heater) immersed in liquid nitrogen. This system can be placed beside a precision balance, such that each deep frozen tube can be tared to zero just before sample transfer.
7. Two runs for 1 min, at 30 beats per second in a TissueLyser, are sufficient to crush *Arabidopsis* seedlings. Tubes should be refrozen in liquid nitrogen between runs. Invert tubes in the second run.
8. Some plant organs can not be crushed completely with TissueLyser. Grind them in a mortar under liquid nitrogen. Mortar grinding requires longer time and at least 400–600 mg per sample.
9. The crushed samples can be stored at −80 °C at least 1 month, without reduction of HMGR activity.
10. Optionally, incubate the samples for 10–20 min at 4 °C in a rotating wheel, at about 15 rpm. This may be required to

completely extract HMGR protein from certain tissues, but long incubation periods should be avoided to prevent HMGR activity loses. We routinely skipped this incubation step with *Arabidopsis* samples.

11. In advance, prepare sufficient volume of RC for the total number of samples to be assayed. Each plant extract and a blank should be assayed in duplicate and two more aliquots of RC (twice 16 μL) should be left to determine the total counts per assay in **step 14** of Subheading 3.4.
12. The final reaction mix contains 24.8 mM Hepes-KOH pH 7.2, 31 mM KCl, 62 mM sucrose, 9.9 mM EDTA, 0.12 % (v/v) Triton X-100, 12.1 mM DTT, 9.3 μg/mL aprotinin, 12.4 μg/mL leupeptin, 2.6 μg/mL E-64, 1.11 μg/mL pepstatin A, 62 μg/mL PMSF, 208 mM Tris–HCl pH 7.2, 50 mM glucose 6-phosphate, 2.5 mM NADP, 0.5 mg/mL BSA, 33.3 μM HMG-CoA, 14.6 μM (77,700 dpm) [3-^{14}C]-HMG-CoA, 0.35 U yeast glucose 6-phosphate dehydrogenase, in a final volume of 42 μL.
13. Incubation time should be adapted to the expected activity. A too long incubation may cause HMGR degradation or substrate shortage. Make sure that mevalonate synthesis is linear with pilot experiments. Mevalonolactone radioactivity higher than 10 % of total counts (about 8,000 cpm in the assayed conditions) likely indicates that the reaction was not linear.
14. After the reaction, open the tubes under the hood. Production of volatile compounds has not been demonstrated in the HMGR activity assays, but is always advisable when running radioactive reactions in complex enzymatic extracts.
15. To start and stop reaction, alternatively to **steps 1–3** (Subheading 3.3), pipette 16 μL of RC to the bottom of the tube (containing 26 μL of extract) at time intervals, close the tube, mix immediately and transfer to a 37 °C water bath. To stop the reaction, add 7 μL of HCl at the same time intervals and mix immediately.
16. Alternatively, freeze the samples down at −20 °C. The process can be interrupted at this point.
17. The flat object should hold the TLC plate below the origin line, such that it does not interfere with the plate loading nor damages the running area.
18. The whole TLC process, including sample application, eluent preparation and plate and chamber handling (**steps 3–7** of Subheading 3.4) should be done under the hood.
19. Prepare the eluent 10–20 min in advance to the run, to allow chamber saturation.

20. Up to three plates can be run at once in a 20 × 20 cm chamber containing seven lateral grooves.
21. Lines A and B delimit the plate area that will contain the mevalonolactone band after migration.
22. Direct contact between the plates and the imaging screen should be avoided. Otherwise, the screen could become contaminated by radioactive material or could be damaged by still remaining HCl.
23. In the recommended TLC system (benzene/acetone 1:1 on silica gel 60), mevalonolactone migrates to an R_f of 0.56–0.58 [45].
24. Counting can be done immediately after adding the scintillation liquid, but this will give lower incorporation and higher variability between replicas.
25. ELISA plates are preferred over individual spectrophotometric cuvettes because less sample volume is required and measurement is done simultaneously for all samples.
26. Dilution should be about 1:10 for *Arabidopsis* seedling extracts obtained as indicated above (2 μL of extraction buffer per mg of tissue). For other plant tissues or other buffer to tissue ratios, appropriate dilutions should be established empirically.
27. We determined plant extract concentration in quadruplicate, with two replicas of the dilution (**step 2** of Subheading 3.5) and two replicas of the measurement of each dilution (**step 3** of Subheading 3.5). Standards were measured in duplicate.
28. The final concentration of the Bradford reagent in the ELISA plate will be one fifth of that in the original stock.
29. According to the Protein Assay manufacturer, absorbance reading can be done 5–60 min after mixing, but we observed that the A_{595} values usually decrease along time, and this can happen at a different rate in the plant extracts and standards. The incubation time should be fixed to better compare the HMGR specific activity between experiments.

Acknowledgment

This work was supported by grants of the Spanish Ministerio de Economía y Competitividad and the Spanish Ministerio de Ciencia e Innovación (BFU2011-24208 to N.C., BIO2009-06984 to A.F. and M.A., and BIO2009-09523 to A.B., including FEDER funds), the Spanish Consolider-Ingenio Program (CSD2007-00036 Centre for Research in Agrigenomics), and the Generalitat de Catalunya (2009SGR0026).

References

1. Rogers DH, Panini SR, Rudney H (1983) Properties of HMGCoA reductase and its mechanism of action. In: Sabine JR (ed) 3-hydroxy-3-methylglutaryl coenzyme A reductase. CRC, Boca Raton, FL, pp 57–75
2. Burg JS, Espenshade PJ (2011) Regulation of HMG-CoA reductase in mammals and yeast. Prog Lipid Res 50:403–410
3. Goldstein JL, Brown MS (1990) Regulation of the mevalonate pathway. Nature 343: 425–430
4. Rodríguez-Concepción M, Campos N, Ferrer A et al (2013) Biosynthesis of isoprenoid precursors in Arabidopsis. In: Bach TJ, Rohmer M (eds) Isoprenoid synthesis in plants and microorganisms: new concepts and experimental approaches. Springer Science + Business Media, New York, pp 459–456
5. Bach TJ (1987) Synthesis and metabolism of mevalonic acid in plants. Plant Physiol Biochem 25:163–178
6. Stermer BA, Bianchini GM, Korth KL (1994) Regulation of HMG-CoA reductase activity in plants. J Lipid Res 35:1133–1140
7. Chappell J (1995) Biochemistry and molecular biology of the isoprenoid biosynthetic pathway in plants. Annu Rev Plant Physiol Plant Mol Biol 46:521–547
8. Vranová E, Coman D, Gruissem W (2013) Network analysis of the MVA and MEP pathways for isoprenoid synthesis. Annu Rev Plant Biol 64:665–700. doi:10.1146/annurev-arplant-050312-120116
9. Brooker JD, Russell DW (1979) Regulation of microsomal 3-hydroxy-3-methylglutaryl coenzyme A reductase from pea seedlings: Rapid posttranslational phytochrome-mediated decrease in activity and in vivo regulation by isoprenoid products. Arch Biochem Biophys 198:323–334
10. Korth KL, Jaggard DAW, Dixon RA (2000) Developmental and light-regulated post-translational control of 3-hydroxy-3-methylglutaryl-CoA reductase levels in potato. Plant J 23:507–516
11. Leivar P, Antolín-Llovera M, Ferrero S et al (2011) Multilevel control of *Arabidopsis* 3-hydroxy-3-methylglutaryl coenzyme A reductase by protein phosphatase 2A. Plant Cell 23: 1494–1511
12. Nieto B, Forés O, Arró M et al (2009) Arabidopsis 3-hydroxy-3-methylglutaryl-CoA reductase is regulated at the post-translational level in response to alterations of the sphingolipid and the sterol biosynthetic pathways. Phytochemistry 70:53–59
13. Wentzinger LF, Bach TJ, Hartmann MA (2002) Inhibition of squalene synthase and squalene epoxidase in tobacco cells triggers an up-regulation of 3-hydroxy-3-methylglutaryl coenzyme A reductase. Plant Physiol 130: 334–346
14. Russell DW, Knight JS, Wilson TM (1985) Pea seedling HMG-CoA reductases: regulation of activity in vitro by phosphorylation and Ca^{2+}, and posttranslational control in vivo by phytochrome and isoprenoid hormones. In: Randall DD, Blevins DG, Larson RL, Kagawa T (eds) Current topics in plant biochemistry and physiology. University of Missouri-Columbia, Missouri, CO, pp 191–206
15. Wititsuwannakul R, Wititsuwannakul D, Dumkong S (1990) Hevea calmodulin: regulation of the activity of latex 3-hydroxy-3-methylglutaryl coenzyme A reductase. Phytochemistry 29:1755–1758
16. Dale S, Arró M, Becerra B et al (1995) Bacterial expression of the catalytic domain of 3-hydroxy-3-methylglutaryl-CoA reductase (isoform HMGR1) from *Arabidopsis thaliana*, and its inactivation by phosphorylation at Ser577 by *Brassica oleracea* 3-hydroxy-3-methylglutaryl-CoA reductase kinase. Eur J Biochem 233:506–513
17. Hemmerlin A (2013) Post-translational events and modifications regulating plant enzymes involved in isoprenoid precursor biosynthesis. Plant Sci 203:41–54
18. Sugden C, Donaghy PG, Halford NG et al (1999) Two SNF1-Related protein kinases from spinach leaf phosphorylate and inactivate 3-hydroxy-3-methylglutaryl-coenzyme A reductase, nitrate reductase, and sucrose phosphate synthase in vitro. Plant Physiol 120:257–274
19. Antolín-Llovera M, Leivar P, Arró M et al (2011) Modulation of plant HMG-CoA reductase by protein phosphatase 2A: positive and negative control at a key node of metabolism. Plant Signal Behav 6:1127–1131
20. Campos N, Boronat A (1995) Targeting and topology in the membrane of plant 3-hydroxy-3-methylglutaryl coenzyme A reductase. Plant Cell 7:2163–2174
21. Denbow CJ, Lang S, Cramer CL (1996) The N terminal domain of tomato 3-hydroxy-3-methylglutaryl-CoA reductases – sequence, microsomal targeting, and glycosylation. J Biol Chem 271:9710–9715
22. Re EB, Brugger S, Learned M (1997) Genetic and biochemical analysis of the transmembrane domain of Arabidopsis 3-hydroxy-3-methylglutaryl coenzyme A reductase. J Cell Biochem 65:443–459

23. Leivar P, González VM, Castel S et al (2005) Subcellular localization of Arabidopsis 3-hydroxy-3-methylglutaryl-coenzyme A reductase. Plant Physiol 137:57–69
24. Merret R, Cirioni JR, Bach TJ et al (2007) A serine involved in actin-dependent subcellular localization of a stress-induced tobacco BY-2 hydroxymethylglutaryl-CoA reductase isoform. FEBS Lett 581:5295–5299
25. Kondo K, Oba K (1986) Purification and characterization of 3-hydroxy-3-methylglutaryl CoA reductase from potato tubers. J Biochem 100:967–974
26. Wititsuwannakul R, Wititsuwannakul D, Suwanmanee P (1990) 3-Hydroxy-3-methylglutaryl coenzyme A reductase from the latex of *Hevea brasiliensis*. Phytochemistry 29:1401–1403
27. Bach TJ, Rogers DH, Rudney H (1986) Detergent-solubilization, purification, and characterization of membrane-bound 3-hydroxy-3-methylglutaryl-coenzyme-A reductase from radish seedlings. Eur J Biochem 154:103–111
28. Choi D, Ward BL, Bostock RM (1992) Differential induction and suppression of potato 3-hydroxy-3-methylglutaryl coenzyme A reductase genes in response to *Phytophthora infestans* and to its elicitor arachidonic acid. Plant Cell 4:1333–1344
29. Chye ML, Kush A, Tan CT et al (1991) Characterization of cDNA and genomic clones encoding 3-hydroxy-3-methylglutaryl-coenzyme A reductase from *Hevea brasiliensis*. Plant Mol Biol 16:567–577
30. Vollack KU, Dittrich B, Ferrer A et al (1994) Two radish genes for 3-hydroxy-3-methylglutaryl-CoA reductase isozymes complement mevalonate auxotrophy in a yeast mutant and yield membrane-bound active enzyme. J Plant Physiol 143:479–487
31. Istvan ES, Palnitkar M, Buchanan SK et al (2000) Crystal structure of the catalytic portion of human HMG-CoA reductase: insights into regulation of activity and catalysis. EMBO J 19:819–830
32. Lynen F (1967) Biosynthetic pathways from acetate to natural products. Pure Appl Chem 14:137–167
33. Hepper CM, Audley BG (1969) Biosynthesis of rubber from β-hydroxy-β-methylglutaryl-coenzyme A in Hevea brasiliensis latex. Biochem J 114:379–386
34. Brooker JD, Russell DW (1974) Some properties of 3-hydroxy-3-methylglutaryl coenzyme A reductase from *Pisum sativum*. Bull Roy Soc New Zeal 12:365–370
35. Suzuki H, Oba K, Uritani I (1974) Occurrence of 3-hydroxy-3-methyl-glutaryl coenzyme A reductase in sweet-potato. Agric Biol Chem 38:2053–2055
36. Huber J, Rudiger W (1978) Subcellular localization and properties of 3-hydroxy-3-methylglutaryl coenzyme A reductase in plant cell suspension cultures of anise. Hoppe-Seylers Z Physiol Chem 359:277–277
37. Douglas TJ, Paleg LG (1978) AMO 1618 effects on incorporation of ^{14}C-MVA and ^{14}C-acetate into sterols in *Nicotiana* and *Digitalis* seedlings and cell-free preparations from *Nicotiana*. Phytochemistry 17:713–718
38. Grumbach KH, Bach TJ (1979) Effect of PSII herbicides, amitrol and SAN 6706 on the activity of 3-hydroxy-3-methylglutaryl-coenzyme A reductase and the incorporation of [2-^{14}C]acetate and [2-^{3}H]mevalonate into chloroplast pigments of radish seedlings. Z Naturforsch (C) 34:941–943
39. Bach TJ, Wettstein A, Boronat A et al (1991) Properties and molecular cloning of plant HMG-CoA reductase. In: Patterson GW, Nes WD (eds) Physiology and biochemistry of plant sterols. American Oils Chemical Society, Champaign, IL, pp 29–49
40. Sipat A (1985) 3-Hydroxy-3-methylglutaryl-CoA reductase in the latex of *Hevea brasiliensis*. Methods Enzymol 110:40–51
41. Sipat AB (1982) Hydroxymethylglutaryl CoA reductase (NADPH) in the latex of *Hevea brasiliensis*. Phytochemistry 21:2613–2618
42. Suzuki H, Oba K, Uritani I (1975) The occurrence and some properties of 3-hydroxy-3-methylglutaryl coenzyme A reductase in sweet potato roots infected by *Ceratocystis fimbriata*. Physiol Plant Pathol 7:265–276
43. Russell DW (1985) 3-Hydroxy-3-methylglutaryl-CoA reductases from pea seedlings. Methods Enzymol 110:26–40
44. Reddy AR, Das VSR (1986) Partial purification and characterization of 3-hydroxy-3-methylglutaryl coenzyme A reductase from the leaves of guayule (*Parthenium argentatum*). Phytochemistry 25:2471–2474
45. Shapiro DJ, Imblum RL, Rodwell VW (1969) Thin-layer chromatographic assay for HMG-CoA reductase and mevalonic acid. Anal Biochem 31:383
46. Young NL, Berger B (1981) Assay of S-3-hydroxy-3-methylglutaryl-CoA reductase. Methods Enzymol 71(Pt C):498–509
47. Chappell J, Wolf F, Proulx J et al (1995) Is the reaction catalyzed by 3-hydroxy-3-methylglutaryl coenzyme A reductase a rate-limiting step for

isoprenoid biosynthesis in plants ? Plant Physiol 109:1337–1343

48. Dai Z, Cui G, Zhou S-F et al (2011) Cloning and characterization of a novel 3-hydroxy-3-methylglutaryl coenzyme A reductase gene from Salvia miltiorrhiza involved in diterpenoid tanshinone accumulation. J Plant Physiol 168:148–157
49. Douglas P, Pigaglio E, Ferrer A et al (1997) Three spinach leaf nitrate reductase-3-hydroxy-3-methylglutaryl-CoA reductase kinases that are required by reversible phosphorylation and/or Ca^{2+} ions. Biochem J 325:101–109
50. Mansouri H, Asrar Z, Mehrabani M (2009) Effects of gibberellic acid on primary terpenoids and D^9-tetrahydrocannabinol in Cannabis sativa at flowering stage. J Integr Plant Biol 51:553–561
51. Toroser D, Huber SC (1998) 3-Hydroxy-3-methylglutaryl-coenzyme A reductase kinase and sucrose-phosphate synthase kinase activities in cauliflower florets: Ca^{2+} dependence and substrate specificities. Arch Biochem Biophys 355:291–300
52. Mozzicafreddo M, Cucciloni M, Eleuteri AM et al (2010) Rapid reverse phase-HPLC assay of HMG-CoA reductase activity. J Lipid Res 51:2460–2463
53. Soto G, Stritzler M, Lisi C et al (2011) Acetoacetyl-CoA thiolase regulates the mevalonate pathway during abiotic stress adaptation. J Exp Bot 62:5699–5711
54. Waldron J, Webster C (2011) Liquid chromatography-tandem mass spectrometry method for the measurement of serum mevalonic acid: a novel marker of hydroxymethylglutaryl coenzyme A reductase inhibition by statins. Ann Clin Biochem 48:223–232
55. Rodríguez-Concepción M, Forés O, Martínez-García JF et al (2004) Distinct light-mediated pathways regulate the biosynthesis and exchange of isoprenoid precursors during *Arabidopsis* seedling development. Plant Cell 16:144–156
56. Closa M, Vranová E, Bortolotti C et al (2010) The *Arabidopsis thaliana* FPP synthase isozymes have overlapping and specific functions in isoprenoid biosynthesis, and complete loss of FPP synthase activity causes early developmental arrest. Plant J 63:512–525
57. Manzano D, Fernàndez-Busquets X, Schaller H et al (2004) The metabolic imbalance underlying lesion formation in *Arabidopsis thaliana* overexpressing farnesyl diphosphate synthase (isoform 1S) leads to oxidative stress and is triggered by the developmental decline of endogenous HMGR activity. Planta 219: 982–992
58. Masferrer A, Arró M, Manzano D et al (2002) Overexpression of *Arabidopsis thaliana* farnesyl diphosphate synthase (FPS1S) in transgenic Arabidopsis induces a cell death/senescence-like response and reduced cytokinin levels. Plant J 30:123–132
59. Pastuszyn A, Havel CM, Scallen TJ et al (1983) (R)3-Hydroxy-3-methylglutaryl coenzyme A: the not-so-innocent bystander in the enzymatic reduction of (S)HMG-CoA to (R) mevalonate. J Lipid Res 24:1411–1411
60. Lalitha R, George R, Ramasarma T (1989) Mevalonate-metabolizing enzymes in *Arachis hypogaea*. Mol Cell Biochem 87:161–170
61. Ram M, Khan MA, Jha P et al (2010) HMG-CoA reductase limits artemisinin biosynthesis and accumulation in *Artemisia annua* L. plants. Acta Physiol Plant 32:859–866
62. Narváez JA, Flores-Pérez P, Herrera-Valencia V et al (2001) Development of molecular techniques for studying the metabolism of carotenoids in Bixa orellana L. Hortscience 36:982–986
63. Harker M, Hellyer A, Clayton JC et al (2003) Co-ordinate regulation of sterol biosynthesis enzyme activity during accumulation of sterols in developing rape and tobacco seed. Planta 216:707–715
64. Kato-Emori S, Higashi K, Hosoya K et al (2001) Cloning and characterization of the gene encoding 3-hydroxy-3-methylglutaryl coenzyme A reductase in melon (Cucumis melo L. reticulatus). Mol Genet Genomics 265:135–142
65. Nishi A, Tsuritani I (1983) Effect of auxin on the metabolism of mevalonic acid in suspension-cultured carrot cells. Phytochemistry 22: 399–401
66. Golbeck JH, Maurey KM, Newberry GA (1985) Detection of 3 hydroxy-3-methylglutaryl coenzyme A reductase activity in *Dunaliella salina*. Plant Physiol 77:48
67. Skrukrud CL, Taylor SE, Hawkins DR et al (1987) Triterpenoid biosynthesis in *Euphorbia lathyris*. In: Stumpf PK, Mudd JB, Nes WD (eds) The metabolism, structure, and function of plant lipids. Plenum, New York, pp 115–118
68. Skrukrud CL, Taylor SE, Hawkins DR et al (1988) Subcellular fractionation of triterpenoid biosynthesis in *Euphorbia lathyris* latex. Physiol Plant 74:306–316
69. Leube J, Grisebach H (1983) Further studies on induction of enzymes of phytoalexin synthesis in soybean and cultured soybean cells. Z Naturforsch (C) 38:730–735

70. Joost O, Bianchini G, Bell AA et al (1995) Differential induction of 3-hydroxy-3-methylglutaryl CoA reductase in two cotton species following inoculation with Verticillium. Mol Plant Microbe Interact 8:880–885
71. Ceccarelli N, Lorenzi R (1984) Growth inhibition by competitive inhibitors of 3-hydroxymethylglutarylcoenzyme A reductase in *Helianthus tuberosus* tissue explants. Plant Sci Lett 34:269–276
72. Bach TJ (1981) Untersuchungen zur Charakterisierung und Regulation der 3-Hydroxy-3-methylglutaryl-Coenzym-A-Reduktase [Hydroxy-methylglutaryl-Coenzym-A Reduktase] (Mevalonat : NADP + Oxidoreduktase, CoA acylierend, E.C. 1.1.1.34) in Keimlingen von Raphanus sativus. Ph.D. Universität Karlsruhe
73. Srinivasan V, Ryu DDY (1992) Enzyme activity and shikonin production in *Lithospermum erythrorhizon* cell cultures. Biotechnol Bioeng 40:69–74
74. Köhle A, Sommer S, Yazaki K et al (2002) High level expression of chorismate pyruvate-lyase (UbiC) and HMG-CoA reductase in hairy root cultures of *Lithospermum erythrorhizon*. Plant Cell Physiol 43:894–902
75. Rupasinghe HPV, Almquist KC, Paliyath G et al (2001) Cloning of *hmg1* and *hmg2* cDNAs encoding 3-hydroxy-3-methylglutaryl coenzyme A reductase and their expression and activity in relation to alpha-farnesene synthesis in apple. Plant Physiol Biochem 39:933–947
76. Arebalo RE, Mitchell ED (1984) Cellular distribution of 3-hydroxy-3-methylglutaryl coenzyme A reductase and mevalonate kinase in leaves of *Nepeta cataria*. Phytochemistry 23:13–18
77. van Deenen N, Bachmann AL, Schmidt T et al (2012) Molecular cloning of mevalonate pathway genes from *Taraxacum brevicorniculatum* and functional characterisation of the key enzyme 3-hydroxy-3-methylglutaryl-coenzyme A reductase. Mol Biol Rep 39:4337–4349
78. Chappell J, Nable R (1987) Induction of sesquiterpenoid biosynthesis in tobacco cell suspension cultures by fungal elicitor. Plant Physiol 85:469–473
79. Gondet L, Weber T, Maillotvernier P et al (1992) Regulatory role of microsomal 3-hydroxy-3-methylglutaryl-coenzyme A reductase in a tobacco mutant that overproduces sterols. Biochem Biophys Res Commun 186:888–893
80. Maurey K, Wolf F, Golbeck J (1986) 3-Hydroxy-3-Methylglutaryl Coenzyme A reductase activity in *Ochromonas malhamensis*: a system to study the relationship between enzyme activity and rate of steroid biosynthesis. Plant Physiol 82:523–527
81. Ji W, Benedict CR, Foster MA (1993) Seasonal variations in rubber biosynthesis, 3-hydroxy-3-methylglutaryl-coenzyme A reductase, and rubber transferase activities in *Parthenium argentatum* in the chihuahuan desert. Plant Physiol 103:535–542
82. Cowan AK, MooreGordon CS, Bertling I et al (1997) Metabolic control of avocado fruit growth – Isoprenoid growth regulators and the reaction catalyzed by 3-hydroxy-3-methylglutaryl coenzyme A reductase. Plant Physiol 114:511–518
83. Cowan AK (2004) Metabolic control of avocado fruit growth: 3-hydroxy-3-methylglutaryl coenzyme a reductase, active oxygen species and the role of C7 sugars. S Afr J Bot 70:75–82
84. Reddy AR, Das VSR (1987) Chloroplast autonomy for the biosynthesis of isopentenyl diphosphate in guayule (*Parthenium argentatum gray*). New Phytol 106:457–464
85. Boll M, Kardinal A (1990) 3-Hydroxy-3-methylglutaryl coenzyme A reductase from spruce (*Picea abies*). Properties and regulation. Z Naturforsch (C) 45:973–979
86. Lütke-Brinkhaus F, Kleinig H (1987) Formation of isopentenyl diphosphate via mevalonate does not occur within etioplasts and etiochloroplasts of mustard *Sinapis alba* L. seedlings. Planta 171:406–411
87. Narita JO, Gruissem W (1989) Tomato hydroxymethylglutaryl-CoA reductase is required early in fruit development but not during ripening. Plant Cell 1:181–190
88. Oba K, Kondo K, Doke N et al (1985) Induction of 3-hydroxy-3-methylglutaryl CoA reductase in potato tubers after slicing, fungal infection or chemical treatment, and some properties of the enzyme. Plant Cell Physiol 26:873–880
89. Josekutty PC (1998) Selection and characterization of *Solanum xanthocarpum* cell line with augmented steroid metabolism. S Afr J Bot 64:238–243
90. Kreuz K, Kleinig H (1984) Synthesis of prenyl lipids in cells of spinach leaf. Compartmentation of enzymes for formation of isopentenyl diphosphate. Eur J Biochem 141:531–535
91. Kim KK, Yamashita H, Sawa Y et al (1996) A high activity of 3-hydroxy-3-methylglutaryl coenzyme a reductase in chloroplasts of *Stevia rebaudiana* Bertoni. Biosci Biotechnol Biochem 60:685–686
92. Post J, van Deenen N, Fricke J et al (2012) Laticifer-specific cis-prenyltransferase silencing affects the rubber, triterpene, and inulin content

of *Taraxacum brevicorniculatum*. Plant Physiol 158:1406–1417

93. Bach TJ, Weber T, Motel A (1990) Some properties of enzymes involved in the biosynthesis and metabolism of 3-hydroxy-3-methylglutaryl-CoA in plants. In: Towers GHN, Stafford HA (eds) Biochemistry of the mevalonic acid pathway to terpenoids. Plenum Press Div Plenum Publishing Corp, New York, pp 1–82